

A PRELIMINARY ASSESSMENT OF A MEDIUM-ENTHALPY GEOTHERMAL RESOURCE IN NAGQU (TIBET)
PEOPLE'S REPUBLIC OF CHINA

Battistelli, A.*., Rivera, R.J.*., D'Amore, F.**, Wu, F.***, Rossi, R.*., and Luzi, C*

* Aquater S.p.A., San Lorenzo in Campo, PS, Italy.

** Istituto Internazionale per le Ricerche Geotermiche, Pisa, Italy.

*** Geothermal Development Corporation of Tibet Autonomous Region, Beijing, PRC.

ABSTRACT

The Nagqu geothermal field is a single-phase, liquid-dominated system at reservoir conditions, having a high gas content. This field is located at an elevation of about 4,500 m (asl), in the vicinity of the City of Nagqu, which is one of the most important cities of Tibet. The reservoir rock is made of a highly fractured, low-permeability sedimentary sequence. During the implementation of the study described in this paper, fluid production was mainly obtained from two out of four possible productive wells. The main fault systems are located in a NE-SW and E-W directions, which seem to control fluid movement at depth. The geothermal field is restricted to a small area where hydrothermal manifestations are located. Reservoir temperature is 114 °C, gas content is in the range of 0.5 to 0.6 percent by mass, being mainly CO₂. Reservoir transmissivity in the area of the wells is very high. Reservoir response to changes in flow rate in any of the producing wells could be detected almost immediately in the observation wells, which were distant between 300 to 900 m, depending on the production-observation well arrangement. Calcium carbonate scaling was present in all producing wells. This deposition was controlled by the CO₂ partial pressure. Description of well testing results is provided, as well as the thermodynamics and geochemistry of reservoir fluids.

INTRODUCTION

The Himalayan Mountain Range is about 250 to 300 km wide and nearly 2,000 km long. There are over 400 areas of active hydrothermal manifestations in the whole zone, including hydrothermal eruptions such as craters, geysers, fumaroles, boiling springs, hot and warm springs, etc.. Surge of geothermal manifestations is strictly controlled by active tectonics.

Nagqu geothermal field is located in Northern Tibet, two kilometers southward of Nagqu Town (see Fig. 1), at an altitude ranging between 4,500 to 4,700 m (asl). The area is characterized by plateau-type morphology with relatively broad flat topography and limited

differences in height (100 to 200 m). Hydrography is well developed in the surroundings of the geothermal field and is represented by the Nagqu River and its tributaries, which originate from the northern mountain area and flow southward into the Nujang water system. The rivers flow rates vary greatly with the seasons. The Giqu river flow rate at Nagqu Town is 69.6 m/s during the rainy period and can be totally absent during the dry season. According to meteorological records from 1981 to 1986 (El. Des. Inst. of SW China, 1989), the annual average temperature is about -2°C, rainfall is about 400 mm and the relative humidity is 50%.

GEOLOGY

Stratigraphy

The basement of the geothermal field is mainly represented by Middle-Jurassic mudstones and sandstones. (Geothermal Geological Team, 1989). In reference to the stratigraphy disclosed by wells, mudstones are prevailing in SW and NE sectors of the geothermal field, mudstone-sandstone interlayerings are prevailing eastward and silicified, fractured sandstone are present in the NW part. Upper Cretaceous magmatic rocks are scattered over the area; they are mainly represented by medium-acidic volcanics, which underwent dynamometamorphism showing laminated and blastic textures; radiometric data revealed ages ranging from 80 to 101 Ma. Neogenic sediments formed by conglomerate in the lower part with sandstone-conglomerate interbeddings in the upper layers outcrop in the area of thermal manifestations. Quaternary deposits are widespread and are represented by the following sequence:

- Lower Pleistocene lake and swamp deposits
- Middle Pleistocene glaciofluvial deposits
- Upper Pleistocene glaciofluvial and alluvium
- Holocene alluvium and diluvium with swampy deposits.

Structure

The most important structural feature in the geothermal field area is represented by an anticline, whose axis trends NE 70° , with dip angle of strata varying from 40 to 60° . After the folding stage, tectonic events of Himalayan stages produced two main faults systems trending NE-SW and E-W: the latter event is older than the NE trend and shows evident compressive characteristics. The NE-SW trending faults are more widespread being produced by tensile stresses. These two tectonic trends have been the most significative alignments in more recent stages of Himalayan tectonics, and even at the present time they represent the active fault belts along which the hydrothermal activity is developed. Moreover, in the area of the geothermal field a NW trend is present which is strictly connected with the geothermal manifestations (Fig. 2), consisting of warm and hot springs, thermal swamps, steaming grounds and deposition of hydrothermal minerals such as kaolinite, silica, pyrite, sulphates and carbonates.

GENERAL BACKGROUND OF FIELD CONDITIONS

A total of 15 exploratory wells have been drilled in the Nagqu Geothermal Field (Fig. 1). Well depth is ranging between 80 and about 400 m, with the exception of wells ZK1005 and ZK1203, drilled down to 503 and 708 m, respectively. Wells ZK1005, 1007, 1105 and 1203 have a 9 5/8" or a 13 3/8" production casing set at depth ranging between 37 and 94 m. Wells ZK1104 and 1303 are completed with both a surface casing and a 9 5/8" production casing, whereas in all remaining wells only a conductor pipe has been installed.

Six wells have been drilled in the productive area, which has a surface of about 600.000 m². Among them well ZK001, the shallowest one, did not reach any productive zone but showed high temperature (about 110°C at 80 m); the other wells, ZK1005, 1104, 1105, 1203 and 1303 are completed with a casing head flange and a master valve as static well head pressure ranging from 3.9 to 5.2 bara is present. Well ZK1105 can not be used for production purposes as it is damaged by a fish with top located at about 104 m. The four productive wells were tested by Chinese experts after drilling completion and for about one week, during a production test of the whole field. During the field survey conducted on this study, only two wells were tested, ZK1203 and 1104. Wells ZK1005 and 1303 were used as observation wells during all field activities.

RESERVOIR FLUID MAIN CHARACTERISTICS

Tables 1 and 2 show the water and gas compositions, respectively.

Table 1. pH value and chemical composition (mg/kg) of reservoir water.

pH	5.8	CO ₂	5240
Na ⁺	1004 (± 23)	HCO ₃ ⁻	2000
K ⁺	66 (± 4)	SO ₄ ²⁻	200
Ca ²⁺	22.5	Cl ⁻	248
Mg ²⁺	6.0 (± 0.7)	F ⁻	8 (± 1)
Al ³⁺	0.035	B	9 (± 0.5)
Fe ²⁺	0.05	NH ₃	6
Li ⁺	2.7	SiO ₂	75

Table 2. Average dry gas composition (Vol %) and gas/water ratio (molar).

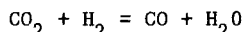
CO ₂	99.5	
H ₂	0.0018	± 0.0006
CH ₄	0.25	± 0.06
CO	0.000005	± 0.000001
H ₂ S*	0.024	± 0.012
N ₂	0.21	± 0.08
Ar	0.0035	± 0.0020
He	0.0013	± 0.0005
gas/(total H ₂ O) = 0.0022		

* A concentration of 0.04% was measured in samples analyzed in the field and is considered as most reliable

As it can be seen from this table, CO₂ is the main component of dissolved gases. Thermo-metamorphism can be considered the main process for the occurrence of CO₂ in this thermal area. Measured ¹³C content of $-1.6 \pm 0.6\%$ confirmed this hypothesis, since a CO₂ concentration of this order can normally be considered as linked to a crustal origin from sediments with no organic or volcanic (mantle) components. This conclusion is supported by the fact that plotting the measured N₂ - Ar - He concentrations on a triangular diagram (Giggenbach et al., 1983) the position of this point is located along the line connecting the meteoric component to the He corner, suggesting a crustal component in the order of 75%.

The carbon monoxide content can be used to estimate the CO₂ partial pressure using the so called water-gas shift reaction (Chiodini

and Cioni, 1989), by making the following chemical equilibrium:



arranging the expression of the equilibrium constant by introducing $P(H_2O)$, the following relation is obtained for a pure liquid phase:

$$\log P(CO_2) = 0.491 + 192.4/T + 0.979 \log T +$$

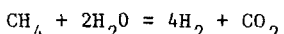
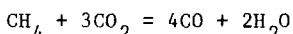
$$\log (CO/H_2) + \log B(CO) - \log B(H_2)$$

where $B(i)$ is the distribution coefficient for each gas species. From gas composition a value of $P_{CO_2} = 11.6$ bar is obtained.

For productive wells, where the gas/(total H_2O) and the reservoir temperature are known, the maximum value of $P(CO_2)$ in the aquifer can be computed, assuming a pure liquid phase, by the following equation:

$$\log P(CO_2) = \log (CO_2/H_2) + \log B(CO_2) + \log P(H_2O)$$

In our case for well ZK1203 a value of 12.8 bar is obtained. Gas composition can be used to compute equilibrium temperature. Two independent chemical equations can be used:



the derived geothermometric equations for a pure liquid phase are:

$$4\log (CO/CO_2) - \log (CH_4/CO_2) = 4.73 - 12913.84/T + 0.719 \log T - 4\log B(CO) + 3\log B(CO_2) + \log B(CH_4)$$

$$4\log (H_2/H_2O) - \log (CH_4/CO_2) + 4\log P(CO_2) = -15.35 - 3952.8/T + 4.635 \log T + 4\log A(H_2) + \log A(CO_2) - \log A(CH_4)$$

where $A(i)$ is a term related to the vapor fraction with respect to total water in the reservoir and the molal distribution coefficient $B(i)$, (D'Amore and Truesdell, 1985). The computed temperature are respectively 110°C and 112°C for a $P(CO_2) = 11.6$ bar. Reservoir fluid temperatures were also computed based upon both the thermal equilibrium of mineral assemblages and the application of some empirical geothermometers.

Computer program WATCH2 (Arnorsson et al., 1982) was used to perform calculations of dissolved species in thermal equilibrium with alteration minerals. Calculated reservoir equilibrium temperature by this method was $118 \pm 6^\circ C$, with the following mineral assem-

blage: kaolinite, calcite, quartz, K-feldspar, Ca-Mg-Na-K montmorillonites, Mg-K-illite, K-mica, Mg-chlorite, fluorite, magnetite and goethite. Most of the minerals used in the mineral assemblage calculations performed have been found in the study of the local aquifer (Geothermal Geological Team, 1989). The low enthalpy of fluids from the Nagqu geothermal system was confirmed by the application of some selected empirical geothermometers (average temperature $125 \pm 9^\circ C$). Using gas composition (CO_2 , H_2S , H_2 and CH_4) and the geothermometer of D'Amore and Panichi (1980) a temperature of $123^\circ C$ was obtained. A summary of results obtained from the application of several empirical geothermometers follows:

Table 4. Computed temperatures with different geothermometers.

Geothermometer	Source	T, °C
Na-K-Ca-Mg	Fournier (1981)	114
Quartz (no steam loss)	Fournier and Potter (1982)	122
K-Mg	Giggenbach et al. (1983)	123
Na-Li	Kharaka et al. (1982)	137
Mg-Li	Kharaka and Mariner (1989)	132

Stable isotopes water composition

For both wells the following average Deuterium and $\delta^{18}O$ contents have been measured for the brine sampled at separation temperature of $96 \pm 1^\circ C$:

$$\delta D = 149.8 \pm 0.5 \text{ (‰ VS. SMOW)}$$

$$\delta^{18}O = 18.0 \pm 0.05 \text{ (‰ VS. SMOW)}$$

Fig. 3 reports measured values as points A. Line B-C represents the local meteoric line drawn using data from Nyingzhong and Yangtixiang thermal areas for cold waters (Aquatier, 1989). Point NZ11 corresponds to a lake located at an altitude of 5,050 m (asl). Point YX8 is the isotopic composition of a river whose recharge area is located at an average altitude of about 5,500 m (asl). On the other hand, line A-D has been drawn considering the theoretical isotopical composition produced by evaporation at $115^\circ C$. No major effects of water-rock interaction have been accounted for considering the low enthalpy of the system. According to this assumption, point D would represent the isotopical composition of meteoric water recharging the geothermal system. Since $\delta^{18}O$ values change of about 0.3 units every 100 m and considering the elevation of YX8 and NZ11, the recharge area indicated by point D has an average elevation of about 5,600 m (asl).

The absence of tritium in the water suggests a long residence time of the meteoric water in the reservoir, with an age exceeding 30 years. Then, we may exclude any mixing with local shallow waters. This can explain the good agreement between measured and computed temperatures using water composition.

Fluid Scaling Tendency

Produced fluids at Nagqu exhibited a high scaling tendency. Scale was made of CaCO_3 mainly. Scaling tendency was evaluated by means of the saturation index, I_S (Corsi, 1986):

$$I_S = \log \frac{[\text{Ca}^{++}] \text{Alk}^2}{P_T \cdot y_{\text{CO}_2}} + 10.22 + 2.739E-2 T - 1.38E-5 T^2 - 1.079E-8 P_T - 2.52 I^{1/2} + 0.919 I$$

where I , $[\text{Ca}^{++}]$ and Alk are expressed in mol/l of water, P_T in Pa and T in $^{\circ}\text{C}$. $I_S > 0$ indicates a supersaturated scaling solution and $I_S < 0$ an undersaturated solution. The mole fraction of CO_2 , y_{CO_2} was calculated from Dalton law:

$$P_{\text{CO}_2} = y_{\text{CO}_2} P_T$$

Calculated I_S value at reservoir conditions was 0.28; meanwhile at atmospheric conditions was 3.45. From these results, it is evident that produced fluid at reservoir conditions is slightly supersaturated, while at the end of the isenthalpic flashing process shows a high scaling tendency. In fact, during the production tests carried out substantial diameter reductions were observed both in the surface lines and downhole.

PRODUCTION TESTING

Carbonate scale deposition, characteristic of productive wells in the Nagqu Field, affects both the production technology and the measurement procedures. As routinely performed in productive wells of the Yangbajing field, located about 220 km south of Nagqu, carbonate scale deposits are mechanically removed using a heavy pipe lowered downhole by means of an electric winch. According to the experience gained in operating Yangbajing power plant, the method is effective for shallow wells when the scale build-up rate is not severe. In Nagqu wells, because of higher CO_2 partial pressure, the scale deposition is quite fast and the mechanical cleaning seems to be necessary each 2 to 4 days.

Production tests were performed during this study using the well known "lip method" established by James (1966). The output curves were determined with 3 production steps that lasted about 2 days each. Before

each step, well ZK1203 was cleaned using the mechanical device, whereas well ZK1104, that produced previously only for testing purposes, was not cleaned. Different lip pipe diameters were used for the 3 steps (4", 5" and 6") on each well. A fourth production step on both wells was carried out mainly for interference test purposes.

During the processing of flow rate data, both the gas content of discharged fluid and the scale build-up at the lip pipe were accounted for, the former being the most important. The gas content in the pre-flashed fluid was estimated to be about 5,300 to 5,700 ppm in wells ZK1203 and 1104, respectively. Published methods to correct the lip pressure readings were applied since the effect of CO_2 partial pressure at lip conditions was proved to be quite high. In fact, although the gas content is not so high if compared with other geothermal fields, its effect becomes important because of low fluid enthalpy. Liquid enthalpy was calculated at flash conditions to be about 470 kJ/kg; thus the vapour phase mass fraction at lip conditions (pressure ranging between 1.10 and 1.79 bara) was very low, between 0.029 to 0.012. The gas mass fraction in the vapour phase was relatively high, ranging from about 0.18 to 0.41, with gas partial pressure between 0.09 to 0.40 bar.

These figures were computed by simulating the isenthalpic fluid flow from conditions at the producing zones, to atmospheric pressure (0.6 bara).

A thermodynamical package based upon the method proposed by Sutton (1976) and updated later by O'Sullivan *et al.* (1985) has been used with minor modifications as an equation of state for the $\text{H}_2\text{O}-\text{CO}_2$ system. To correct the lip pressure readings several methods were tested: James (1970), Karamarakar and Cheng (1980), Grant *et al.* (1982a) and Grant *et al.* (1982b). The first three proved to be quite consistent in the range of measured lip pressures, whereas the last one gave a higher correction. It was decided to use the method suggested by Karamarakar and Cheng, as it is based on a theoretical assessment of James' method made using two-phase flow models at the lip pipe. According to this method, correction to measured lip pressures are as follows:

$$P_{\text{lip}}^c = P_{\text{lip}} (1 - Y/m)$$

where:

Y = ratio between the mass of gas and steam in the vapour phase at lip conditions;

$$m = 2.4 - 9.6E-4 (P_{\text{lip}} - P_{\text{atm}}) + Y$$

Corrected lip pressures were about 92 % and 77 % of original readings at lip pressures of 1.10 and 1.79 bara, respectively.

Another factor influencing flow rate measurements was the scale build-up inside the

lip pipe. Average scale thickness measured after two days of production was ranging between 2 and 7 mm; the thickness was higher in the smaller diameters. As a first approximation, a linear increase in scale thickness during production steps was considered to evaluate the actual lip pipe inside diameter to be used in James' equation.

PRODUCTION TESTS RESULTS

Production output curves determined on wells ZK1203 and 1104 are shown in Fig. 4 (Aquater, 1990).

The effect of non-condensable gases is evident in Fig. 5 where pressure profiles recorded in well ZK1203 under static conditions and during production steps of the output curve are plotted. Two-phase flow is clearly present above 100 m during the highest tested flow rate.

Temperature profile T3 recorded at the same time of P3 is also shown. The profile shows the quite uniform temperature distribution down to 700 m, with temperature ranging between 111.5 to 113 °C.

The effect of CO₂ content on boiling pressure can easily be seen in Fig. 6. It illustrates P-T data collected during dynamic surveys at well ZK1203, compared with the pure water saturation line if no dissolved gases were present. Taking into account the accuracy of P-T measurements, the departure from a nearly isothermal flow can be detected at a total pressure of about 14.5 ± 1.0 bara. Good agreement is obtained with the data measured in well ZK1104, which indicated a boiling pressure of about 16.0 ± 1.0 bara as well as with the values obtained through the processing of chemical data. The CO₂ partial pressure at boiling conditions is between 8 and 9 times the steam pressure, which is not a very common feature.

WELL TESTING

Pressure buildup tests

For the characterization of the reservoir, buildup tests were conducted at the two producing wells. Downhole pressure changes were measured by means of mechanical, Ametradia-type pressure sensing-recording devices. An extremely fast pressure recovery was observed in all tests performed, which coupled with the limited accuracy of the mechanical type of sensors used, did not allow the recording of enough quality data to perform either adequate type-curve or semilog analyses.

Heavy leaks of fluids at the wellhead prevented a complete shut-in of the wells, and increased the difficulty of the analysis of the well tests.

Preliminary diagnosis analyses by means of log-log plots of both pressure-difference vs.

time and pressure derivative function vs. time were performed. Matching of pressure-difference vs. time data to type-curve was not feasible due to the extremely short stabilization period and also the small range of pressure differences involved. On the other hand, matching of the pressure derivative function vs. time was not either possible due to the large scatter of data points even after performing several attempts of pressure derivative calculation using different smoothing parameters. Fig. 7 shows data from one of these tests. Type curves published by Bourdet *et al.* (1984) were used.

Interference Tests

To carry out interference tests, the two extreme wells ZK1005 and ZK1303 were chosen as observation wells, while internal wells ZK1104 and ZK1203 were active wells (see Fig. 1). Wellhead pressures and smoothed production data during the test are shown in Fig. 8. To ensure that wellhead measurements would provide reliable data, recordings of such measurements on well ZK1303 for one week previous to the start of the interference test were carried out, excluding in this way the possible effect of any gaseous column inside the well.

Interpretation of interference tests was carried out by means of type-curve matching procedures, using both a homogenous system and a naturally-fractured reservoir system models, applied to pressure response produced by a single production step, without accounting for the effect of previous steps.

A) Type-curve matching using a model for a homogenous system.

For this purpose, the type-curve for a homogeneous system published by Ramey (1980) was used. Interpretation equations for this model are as follows (nomenclature at the end of paper):

$$kh = 141.2 q \mu B (P_D / \Delta P)_M$$

$$\phi_t h = \frac{0.000264 k h}{\mu r^2} \left(\frac{\Delta t}{t_D / r_D} \right)_M^2$$

Units in these eqs. are: k(md), h(ft), q(STB/day), P(Psi), B(STB/bbl), μ (cp), r(ft), t(hr), ϕ (fraction).

Fig. 9 shows the match of field data with the published type curve obtained for test period IT2 shown in Fig. 8. Table 4 below shows results obtained from matches during flow periods IT1 through IT3 of Fig. 8.

B) Type - curve matching using a double - porosity, naturally fractured system model.

Taking into account that from geological

Table 4. Results of field data matching with a homogenous reservoir model.

FLOW PERIOD	kh (d m)	ϕc_t^h (m bar ⁻¹)
IT1	402.1	269 E-5
IT2	455.7	343 E-5
IT3	338.5	53 E-5

evidence, reservoir rock consists of fractured-sedimentary rock, the use of a naturally fractured, double-porosity model seems justified. The model published by Deruyck *et al.* (1982) was used for the interpretation. It was found that the model that assumes transient interporosity flow between the system of fractures and the matrix blocks, better fitted measured field data and so it was the one selected.

Interpretation equations are as follows:

a) For the log-log analysis:

$$k_f^h = 141.2 q B \mu (P_D / \Delta P)_M$$

$$(\phi V c_t)_f^h = \frac{0.000264 k_f^h}{\mu r^2} \frac{\Delta t}{t_D^2 / r_D^2}$$

$$(\phi V c_t)_{f+M}^h = \frac{(\phi V c_t)_f^h}{\omega}$$

b) For the semilog analysis

$$k_f^h = \frac{162.6 q B \mu}{m}$$

$$(\phi V c_t)_{f+M}^h = \frac{k_f^h}{\mu r^2} 10^{-a}$$

$$a = \frac{P_{lh}}{m} + 3.23$$

Fig. 10 illustrates the match obtained for data from period IT2. A summary of results of fitting field data with the published type-curve is given in Table 5, below.

Fig. 11 shows a semilog plot of data from period IT2. From the slope of the straight line in this figure the following values for reservoir parameters are obtained:

$$k_f^h = 288 \text{ (d m)}$$

Table 5. Results of field data matching with a double - porosity, naturally fractured system model.

Flow Period	k_f^h (d m)	ω	$(\phi V c_t)_{f+M}^h$ (m bar ⁻¹)
IT1	287	1.0 E-2	100 E-4
IT2	314	1.5 E-2	174 E-4
IT3	299	*	*

* The test was too short and no response from the matrix was yet evident.

$$(\phi V c_t)_{f+M}^h = 68.2 E-4 \text{ (m bar}^{-1}\text{)}$$

As it can be seen by comparison with results of the type-curve matches given in Table 5, the k_f^h value calculated with the semilog method agrees well with those calculated by the type-curve procedure; meanwhile, the storativity value is somehow lower. Therefore, it can be concluded that the high transmissivities obtained from the type-curve analysis, confirm the presence of a highly fractured system, with transmissivity ranging between 338 to 456 d m if a homogenous system model is assumed or from 287 to 314 d m if a naturally fractured system model is considered. Based upon geological evidences, the latter seems to be more realistic. In this model the fracture system acts as the main fluid conduits, while the matrix represents the main source of fluid storage.

FITTING OF INTERFERENCE DATA USING SIMPLE LUMPED PARAMETER MODEL

As can be seen in Fig. 8, the response of two observation wells seems to be very similar. The two sets of data showed a linear relationship with a unit slope and a standard deviation of 0.0099 bar. This result suggests that the effect of fluid extraction was to produce a quite uniform decline of pressure throughout the reservoir. In this case the use of lumped parameter models to interpret the interference data was considered suitable.

As a first approach the assumption of a steady state recharge to the reservoir from a supporting aquifer was evaluated according to the Schiltuis equation (Olsen, 1984). In this approach a mass balance takes into account three main contributions: the fluid produced from the system, the recharge to the system, and the liquid expansion in the reservoir due to the lowering of average reservoir pressure.

According to the Schiltuis assumption the water recharge is directly proportional to the pressure drawdown in the reservoir. The

aquifer will supply any rate extracted by the wells after an initial drawdown during which there is a pressure decline depending on the rate of production and reservoir storage coefficient. According to the conceptual reservoir model, the vertical recharge through faults and highly fractured zones was modeled considering a linear aquifer recharging the reservoir. Examining the results, it was concluded that this model was not able to provide a good fit of field data.

Next approach was to consider fluid recharge to the reservoir under transient conditions. Under these conditions reservoir behaviour is described by a material balance equation and a simplified solution to the diffusivity equation. The solution used was that presented by Hurst (Olsen, 1984 - Brock, 1986) for an infinite linear aquifer recharging the reservoir.

The characteristic parameter defined by Hurst for a linear system is a ratio of aquifer and reservoir parameters and a geometric factor. It is defined as follows:

$$\lambda = \frac{c_a \mu_a}{l c_r \mu_r}$$

The general solution to be used is as follows:

$$P_0 - P(t_n) = B \sum_{j=0}^n \Delta w_j M(\lambda^2 (t_D - t_{Dj}))$$

where:

$$M(\lambda^2 t_D) = \frac{1}{\lambda^2} (e^{\lambda^2 t_D} \operatorname{erfc}(\lambda \sqrt{t_D}) -$$

$$\frac{2 \lambda \sqrt{t_D}}{1 + \frac{\lambda^2 t_D}{\pi^{0.5}}}$$

$$t_D = \frac{k_a}{\phi_a \mu_a c_a} t$$

for a linear infinite reservoir;

$$B = \frac{\mu_a c_a}{k_a v \theta_R c_R}$$

For a given value of λ parameter, it is possible to determine the B parameter through a linear regression analysis using the least square criterion. The standard deviation of calculated pressure drops respect to the measured ones is determined at the same time. The solution is represented by the couple $B-\lambda$ that gives the minimum standard deviation. Considering the data recorded at Nagqu field, the plot of standard deviation vs. λ does not show any minimum but it stabilizes around 0.023 bar for λ greater than about 0.1 m^{-1} , slowly decreasing for $\lambda \rightarrow \infty$.

As pointed out by Brock (1986), under these conditions it is not possible to determine reservoir parameters, but by using a high value of λ in the flattened part of the curve, a history match and a prediction can still be performed. Under these conditions, the size of the reservoir can be considered as small compared with the size of the system (reservoir+aquifer), so that the reservoir has practically no influence in determining the system behaviour. Although this fact seems to be in good agreement with geological data suggesting a limited reservoir extension, it must be recognized that production period was short and that perhaps data collected under longer production history could show some features not evident during the period tested.

The history match is shown in Fig. 12, where calculated and measured pressures are plotted. Even if the history match can be considered satisfactory from the point of view of matching accuracy (standard deviation was 0.023 bar), the interpretation still has to be considered as a preliminary one. In fact, the interference test covers a short period of about 580 hours and a small amount of fluid extracted, about 48.6 Mkg, with a maximum pressure drawdown of only 0.43 bar.

PRELIMINARY ASSESSMENT OF RESULTS

Eventhough the reservoir is liquid dominated, the high partial pressure of non-condensable gases can be very important in determining both the natural reservoir state and future reservoir behaviour under exploitation. From analysis of data collected, it is evident that in the central part of the field, where vertical upflow of fluid at nearly constant temperature is present, boiling conditions should be reached at depths ranging from 100 to 120 m. This means that a two-phase zone could evolve in the upper part of the reservoir. If this two-phase shallow zone should be present, the reservoir compressibility would be higher than that coming from a liquid phase only, because of liquid vaporization as pressure decreases. This mechanism could furnish a support to pressure stabilization in addition to that supplied by the recharging aquifer.

The above mentioned mechanism could be important in altering reservoir behaviour respect to that of a pure liquid phase in case of long term industrial production. A mass rate extraction of about 80 kg/s has been estimated necessary to produce about 0.9 MWe with an air cooled binary cycle plant. The continuous extraction at this level could produce an important reservoir depletion, extending downwards the two-phase zone.

To properly assess the feasibility of the preliminary results obtained in this study, longer production tests at rates close to 80 kg/s should supply additional data very helpful in assessing long term reservoir behaviour under industrial exploitation level

rates.

CONCLUSIONS

Based upon the analysis of the data collected from the tests performed at wells from the Nagqu Geothermal Field and the analyses performed at the fluid samples collected, the following conclusions can be withdrawn:

1. The area of geothermal field and its surroundings do not present any evidences of volcanic activity able to produce an anomalous thermal gradient. According to the values achieved with drilling, it can be noted that the thermal gradient decreases sharply outside the area of producing wells; furthermore the values of the thermal gradient are controlled by structural trends. In fact wells ZK1403 and ZK903 located 0.8 to 1.2 km respectively away from producing wells show gradients varying from 4.2 to 7.6 °C/100 m, while ZK807 located 2 km away from productive wells, but closer to an active tectonic trend shows a gradient of 14.5 °C/100 m (Geothermal Geological Team, 1989). The producing wells tested practically exhibit no gradient, with temperature almost constant from about 200 m down to total depth and values between 113 to 115°C. This fact demonstrates the uprise of geothermal fluids along fault planes and lack of anomaly far from those planes. Crustal origin of dissolved gases is a further demonstration of the absence of any magmatic-type heat source.

2. According to the data provided by the Geothermal Geological Team (1989), cap rock and reservoir formations can not be distinguished. In fact the Quaternary deposits does not present any cover characteristics; below these depositions, drilling of geothermal wells crossed mainly Jurassic formations represented by mudstone, siltstone and sandstone with very low to null primary permeability. Tectonic activity can produce fractured sandstone layers, which can act as storing levels for geothermal fluids; but limited lateral extension of such layers away from the faults, confines the interest of these reservoirs to the surroundings of the active faults. Such a conclusion is proved to be valid by the thermal gradient distribution obtained in the drilled wells.

3. The reservoir tapped by means of the wells drilled at the Nagqu field corresponds to a liquid dominated reservoir containing compressed water at a measured temperature between 113 and 115 °C. Estimated reservoir fluid temperatures from water rock equilibria and empirical geothermometers are in good agreement with measured temperature.

4. Produced fluids at the surface are two-phase with a steam content in the order of 5% at atmospheric conditions, and high gas content of about 5,500 ppm in total fluid.

The pH in the reservoir has been computed as 5.8. Water is bicarbonate-alkaline and shows a strong scaling nature with deposition of CaCO_3 .

5. From the behaviour shown by the reservoir during the interference test performed, a reservoir volume of limited extension could be inferred.

6. Matching of measured data by means of lumped-parameter models have shown that pressure drawdown in the reservoir under exploitation will be dependent on aquifer recharge. Recharge in the reservoir seems to be controlled by the uplift of hot fluids through vertical fractures.

7. Results obtained from the interpretation of the well testing program carried out in the field have shown that the reservoir behaves as a high-permeability, double porosity, naturally fractured system.

8. Preliminary forecast of future reservoir behaviour based upon the small amount of production data available and the high gas content, indicates that pressure drawdown at the reservoir induced by exploitation, could favour the evolution of a two-phase zone in the upper portion of the reservoir, as exploitation time proceeds.

9. For the two producing wells tested, the flashing zone under the flow rates ranges covered in determination of the characteristic production curves, was located between 100 and 130 m (from ground level).

10. The estimated boiling pressure ranges between 14.5 to 16.0 \pm 1.0 bara.

11. A crustal origin has been identified for gas produced from both, the ^{13}C content in CO_2 and the relative position of the produced gas composition in a $\text{H}_2\text{-N}_2\text{-He}$ diagram.

12. An underground circulation time greater than 30 years for the produced fluid was confirmed from the absence of tritium in fluids sampled. Departure of δD vs. $\delta^{18}\text{O}$ data from the meteoric straight line can be explained by a steam loss from the reservoir prior to well production. Presence of numerous small thermal manifestations all over the field seem to confirm this conclusion.

ACKNOWLEDGEMENTS

The authors wish to acknowledge the U.N.D.P. (D.T.C.D.) and the Geothermal Development Corporation of Tibet Autonomous Region (PRC) for permission to publish this paper, and the Nagqu Prefecture Administration for its help in solving all logistic problems during field activities implementation.

NOMENCLATURE

Alk	alkalinity, mol/l
B	formation volume factor, m^3/m^3 (STB/bbl)
B(i)	distribution coefficient of gas i, dimensionless
c	compressibility, Pa^{-1} (psi^{-1})
h	producing formation thickness, m (ft)
I	ionic strength, $mol\ l^{-1}$
Is	saturation index, dimensionless
k	permeability, m^2 (d m)
l	reservoir thickness, m (ft)
m	correction factor in Karamarakar equation, dimensionless
	slope from the semilog straight line, bar/cycle ($psi/cycle$)
P	pressure, bar (psi)
Patm	atmospheric pressure, bara
Plip	lip pressure, bara
P _T	total pressure, Pa
q _I	volumetric flow rate, m^3/h (STB/d)
Y	gas/steam ratio at lip conditions, dimensionless
Y _{CO2}	molar fraction of CO_2 in the vapor phase
Y _s	steam/total water ratio, fraction
r	radius, m (ft)
t	time, s (hr)
V	volume, m^3
X	mole fraction
φ	porosity, fraction
λ	Hurst parameter, m^{-1}

μ	water dynamic viscosity, Pa s (cp)
ρ	density, kg/m ³
ω	storativity ratio, dimensionless
Main subscripts:	
a	aquifer
c	corrected
D	dimensionless
f	fracture
M	matrix
r	reservoir
t	total

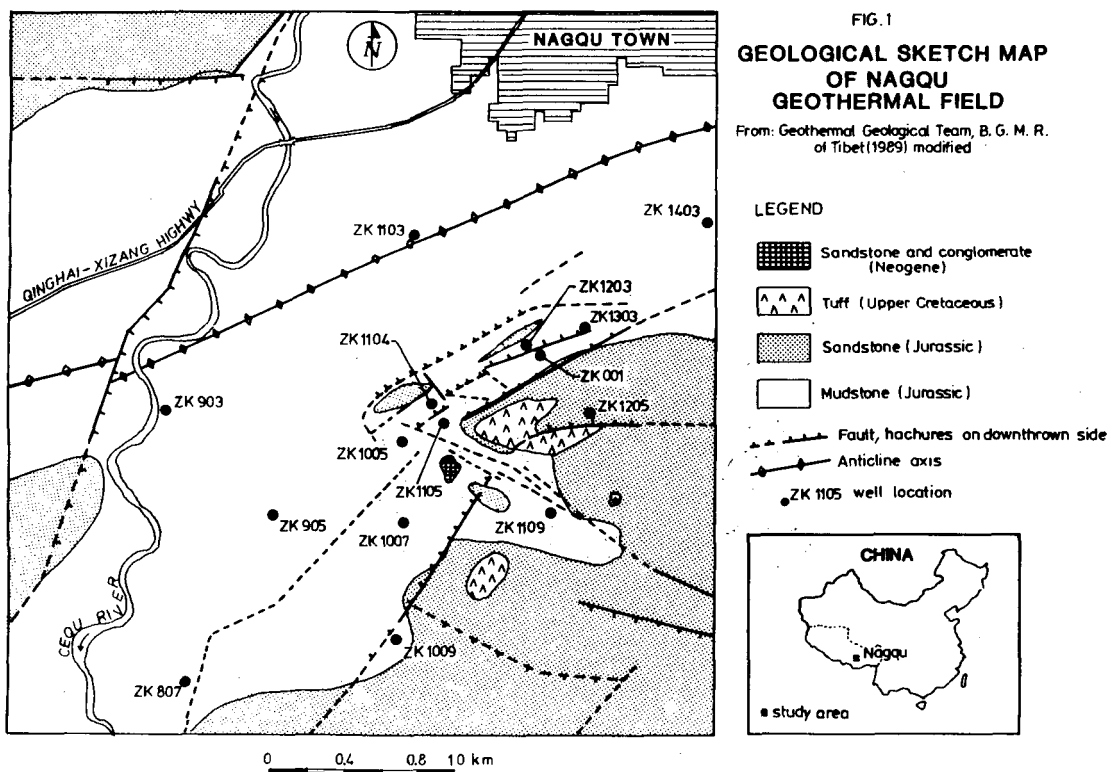
REFERENCES

Aquater, 1989, "Preliminary Technical Report", U.N.D.T.C.D. Contract N. TCD-CON 9/89. Project N. CPR/88/007, unpublished report.

Aquater, 1990, "Engineering Services in the Nagqu Geothermal Field of Tibet (PRC)", U.N.D.T.C.D. Contract N. TCD-CON 9/89. Project N. CPR/88/007, unpublished report.

Arnórsson, S., Sigurðsson, S. and Svavarsson, H., 1982, "The chemistry of geothermal waters in Iceland. I. Calculation of aqueous speciation from 0° to 370°C", Geochim. Cosmochim. Acta, 46, pp. 1513-1532.

Baines, I., Irwin, W.P. and White, D.E., 1978, "Global distribution of carbon dioxide discharges and major zones of seismicity", U.S.G.S. Report, Water Resources Investigation, pp. 78-79.



Bourdet, D.P., Ayoub, J.A. and Pirard, Y.M., 1984, "Use of Pressure Derivative in Well Test Interpretation", Paper SPE 12777, presented at the 1984 Cal. Reg. Meet., Long Beach, CA, April 11-13, 1984.

Brock, D.C., 1986, "Compressibility Effects in Modeling Two-Phase Liquid Dominated Geothermal Reservoirs", SGP-TR-102, Stanford University, Stanford, CA.

Chiodini, G. and Cioni, R., 1989, "Gas geobarometry for hydrothermal systems and its application to various Italian geothermal areas", *Appl. Geochem.*, 4, pp. 455-464.

Corsi, R., 1986, "Scaling and corrosion in geothermal equipment: problems and preventive measures", *Geothermics*, Vol. 14, N. 5/6, pp. 839-856.

D'Amore, F. and Panichi, C. 1980, "Evaluation of deep temperatures of hydrothermal systems by a new gas-geothermometer", *Geoch. Cosm. Acta*, 44, pp. 549-556.

D'Amore, F. and Truesdell, A.M., 1985, "Calculation of geothermal reservoir temperatures and steam fractions from gas compositions", *Geoth. Res. Coun. Trans.*, 9, Part 1, pp. 305-310.

D'Amore, F., Fancelli, R., Saracco, L. and Truesdell, A.H., 1987, "Gas geothermometry based on CO content. Application in Italian Geothermal Fields", 12th Workshop on Geoth. Res. Eng., Stanford University, Stanford, CA, pp. 247-252.

D'Amore, F. and Truesdell, A.H., 1988, "A review of solubilities and equilibrium constants for gaseous species of geothermal interest", *Sci. Géol. Bull. Strasbourg*, 41, 3-4, pp. 309-332.

Deruyck, B.G., Bourdet, D.P., Da Prat, G. and Ramey, H.J. Jr., 1982, "Interpretation of Interference Tests in Reservoirs with Double Porosity Behaviour-Theory and Field Examples", Paper SPE 11025 presented at the 57th Annual Fall Tech. Conf. and Ex. of the SPE of AIME, New Orleans, LA, Sept. 26-29, 1982.

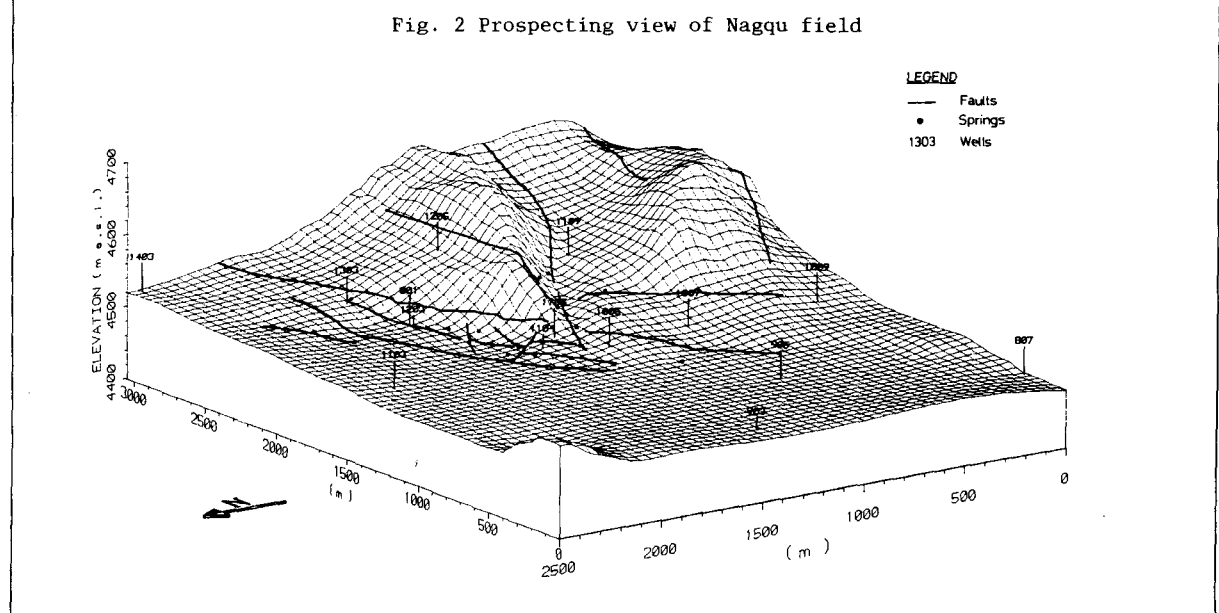
Electricity Designing Institute of Southwestern China, 1989, "Report on Feasibility of Constructing Nagqu Geopower Station, Xizang (Tibetan) Autonomous Region, P. R. China", Index No. F075K, Ministry of Energy, Chengdu, Sichuan Province, unpublished report.

Fouillac, C., and Michard, G., 1981, "Sodium/lithium ratio in water applied to the geothermometry of geothermal waters", *Geothermics*, v.10, pp. 55-70.

Fournier, R.O., 1981, "Application of water geochemistry to geothermal exploration and reservoir engineering", Chapt. 4 in *Geothermal Systems: Principles and Case Histories*, L. Ryback and L.J. P. Muffler eds. Wiley New York, pp. 109-143.

Fournier, R.O., and Potter, R.W., 1982, "A revised and expanded silica (quartz) geothermometer", *Geoth. Res. Couns. Bull.*, v. 11, pp. 3-9.

Fig. 2 Prospecting view of Nagqu field



Geothermal Geological Team, 1989, "The report on the Feasibility Study of Nagqu Geothermal Field, Tibet, P. R. China", Bureau of Geology and Mineral Resources of Tibet, unpublished report.

Giggenbach, W.F., Gonfiantini, R., Jangi, B.L. and Truesdell, A.H., (1983), "Isotopic and chemical composition of Pazabati valley geothermal discharges, north-west Himalaya, India", *Geothermics* 12, pp. 199-222.

Giggenbach, W.F. and Goguel, R.L., 1989, "Collection and analysis of geothermal and volcanic water and gas discharges", New Zealand D.S.I.R. Report n. cd 2401, pp. 1-81.

Grant, M. A., Donaldson, I. G. and Bixley, P. F., 1982a, "Geothermal Reservoir Engineering", Academic Press.

Grant, M. A., James, R. and Bixley, P. F., 1982b, "A Modified Gas Correction for The Lip Pressure Method", Proc. 8th Workshop Geoth. Res. Eng., Stanford University, Stanford, CA.

Helgeson, H.C., Delany, J.M., Nesbitt, H.W. and Bird, D.K., 1978, "Summary and critique of the thermodynamic properties of rock-forming minerals", Am. J. of Sci., 278-A, pp. 1-229.

James, R., 1966, "Measurements of Steam-Water Mixtures Discharging at the Speed of Sound to the Atmosphere", New Zealand Eng., Vol. 2, Part 2, pp. 1676.

James, R., 1970, "Factors Controlling Borehole Performance", U.N. Symp. on the Dev. and Ut. of Geoth. Res., Pisa, *Geothermics*, Vol.

2, Part 2.

Karamarakar, M. and Cheng, P., 1980, "A Theoretical Assessment of James' Method for the Determination of Geothermal Wellbore Discharge Characteristics", *Geoth. Res. Eng. Manag. Progr.*, LBL-11498, GREMP-12, UC-66a.

Kharaka, Y.K., Lico, M.S. and Law, C.M., 1982, "Chemical geothermometers applied to formation waters, Gulf of Mexico and California Basins (ABS.)", Am. Assoc. Petrol. Geol. Bull., 66, 588.

Kharaka, Y.K. and Mariner, R.H., 1989, "Chemical geothermometers and their application to formation waters from sedimentary basins", in Naeser N.D. and McCollom T.M. (EDS.), Thermal history of sedimentary basins, Springer-Verlag, New York, pp. 99-117.

Olsen, G., 1984, "Depletion Modeling of Liquid Dominated Geothermal Reservoirs", Master's Report, Stanford University, Stanford, CA..

O'Sullivan, M. J., Bodvarsson, G. S., Pruess, K. and Blakeley, M. R., 1985, "Fluid and Heat Flow In Gas-Rich Geothermal Reservoirs", Soc. of Pet. Eng. J., Apr. 1985, 215-226.

Ramey, H.J. Jr., 1980, "A Drawdown and Buildup Type - Curve for Interference Testing", 3rd Int. Well Test Symp., LBL, UC.

Sutton, F. M., 1976, "Pressure-temperature curves for a two-phase mixture of water and carbon dioxide", New Zealand J. of Sci., Vol.19, 297-301.

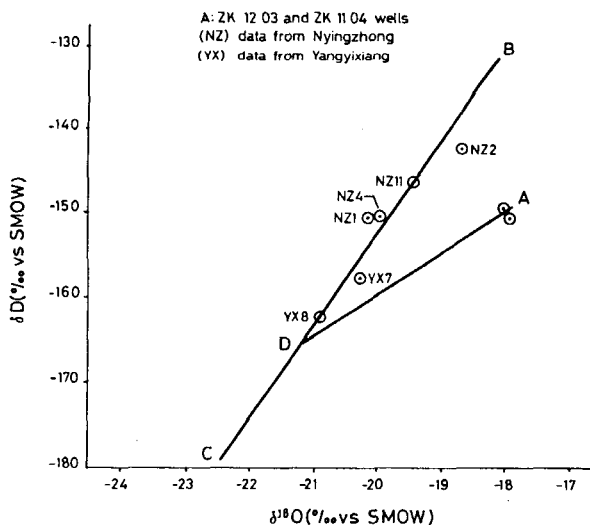


Fig. 3 Stable isotopes water composition

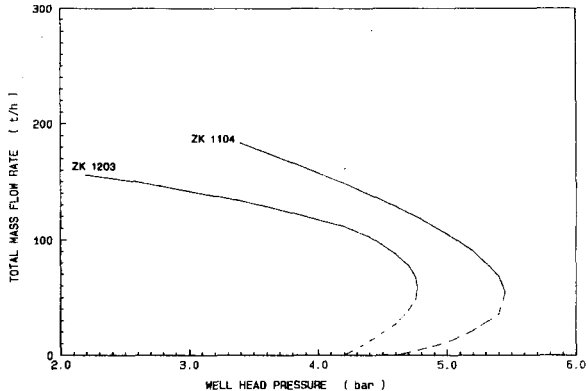


Fig. 4 Output curves of wells ZK 1104 and ZK 1203

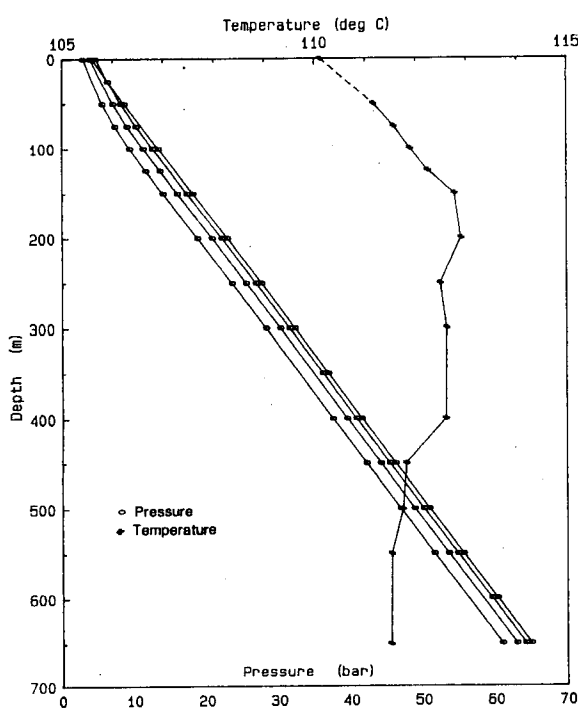


Fig. 5 Measured pressure and temperature profiles of well ZK 1203

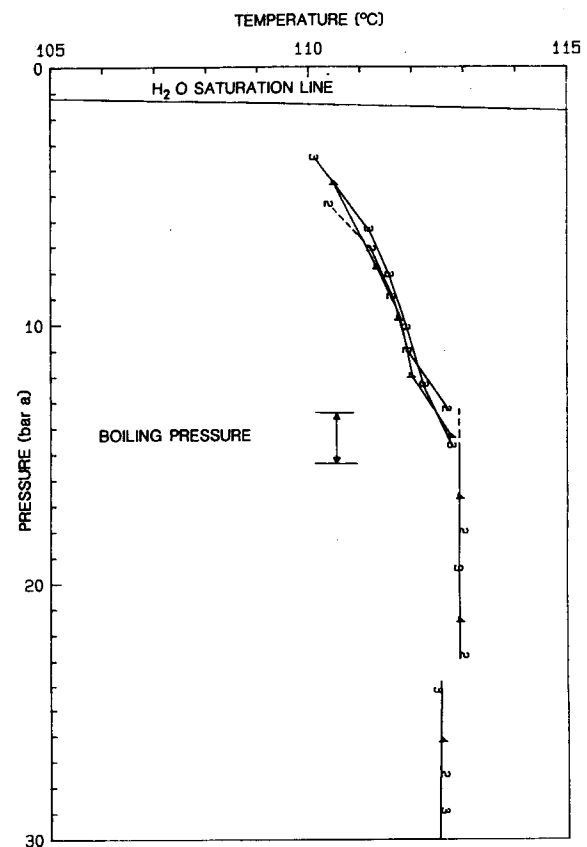


Fig. 6 Pressure-temperature data measured at well ZK 1203 compared with the H_2O saturation line

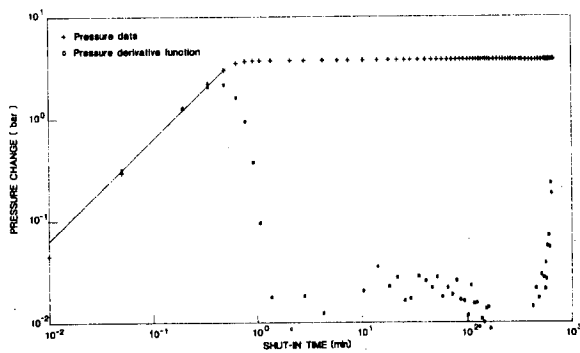


Fig. 7 Composite plot of pressure change and pressure derivative function vs. time for a build-up test performed at well ZK 1203 after IT1 production step

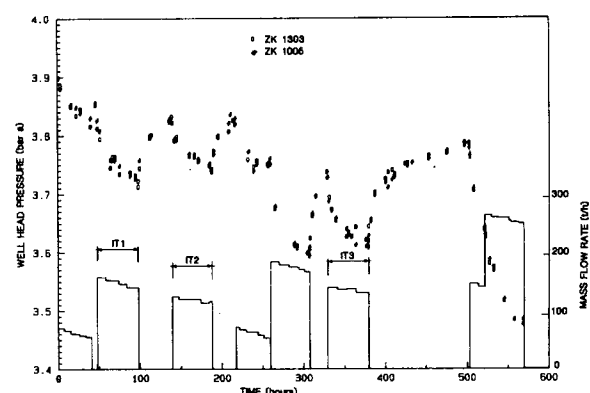


Fig. 8 Well head pressure and smoothed production history vs. time

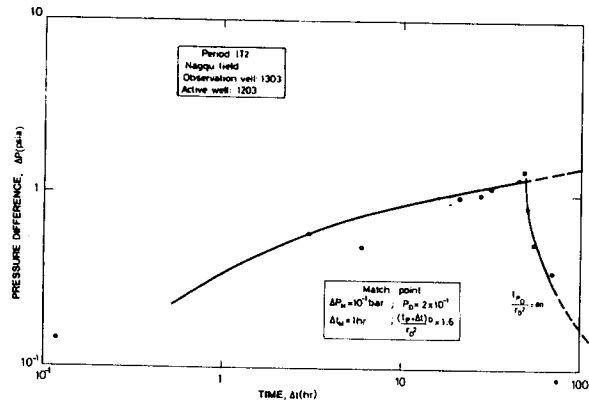


Fig. 9 Type curve match of data from period IT2 by means of a homogeneous model

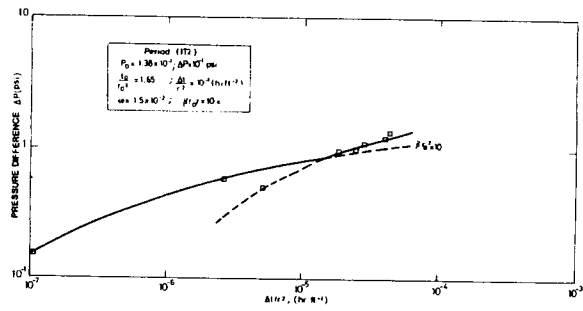


Fig. 10 Type curve match of data from period IT2 by means of a naturally-fractured, double porosity model

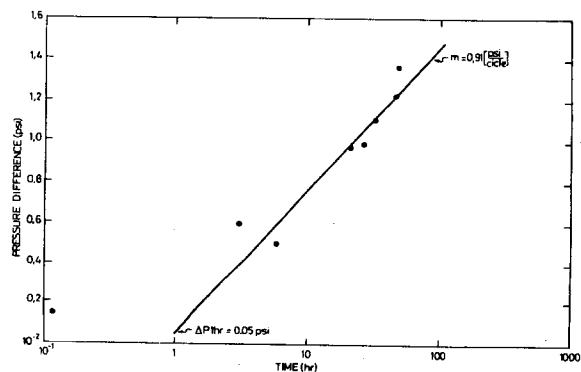


Fig. 11 SEMILOG ANALYSIS OF DATA FROM PERIOD IT2

Fig. 11 Semilog analysis of data from period IT2

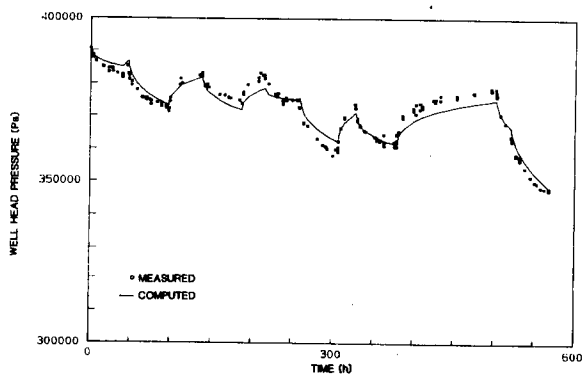


Fig. 12 Well head pressure data match using the lumped parameter model with water recharge according to Hurst simplified model